

Upper critical field of the magnetic superconductor $\text{RuGd}_{1.4}\text{Ce}_{0.6}\text{Sr}_2\text{Cu}_2\text{O}_{10-\delta}$

M. T. Escote, V. A. Meza, and R. F. Jardim*

Instituto de Física, Universidade de São Paulo, Caixa Postal 66318, 05315-970 São Paulo, Brazil

L. Ben-Dor

Department of Inorganic and Analytical Chemistry, Hebrew University, Jerusalem 91904, Israel

M. S. Torikachvili

Department of Physics, San Diego State University, San Diego, California 92182-1233

A. H. Lacerda

National High Magnetic Field Laboratory (NHMFL), Los Alamos National Laboratory, Los Alamos, New Mexico 87545

(Received 17 April 2002; revised manuscript received 5 August 2002; published 14 October 2002)

We performed measurements of magnetic susceptibility, electrical resistivity, and magnetoresistance in magnetic fields of up to 18 T in the magnetic superconductor $\text{RuGd}_{1.4}\text{Ce}_{0.6}\text{Sr}_2\text{Cu}_2\text{O}_{10-\delta}$ synthesized in oxygen pressures up to 95 atm. The magnetic-susceptibility data show the occurrence of an antiferromagnetic state below $T_N \sim 175$ K, followed by the development of a weak ferromagnetic state near $T_M \sim 100$ K, and followed further by the onset of superconductivity (SC) at $T_c \sim 42$ K. The electrical resistivity as a function of temperature shows an evolution from nonmetal-to-SC behavior in samples prepared in a flux of O_2 to a well defined metal-like behavior in samples prepared under 95 atm pressure of O_2 . The electron-phonon coupling constant was calculated from transport data to be $\lambda_{tr} \sim 0.17$, a value comparable with other cuprates, indicating weak electron-phonon coupling in these ruthenates. The values of the upper critical field H_{c2} for the O_2 high-pressure treated samples were obtained from the magnetoresistivity data yielding $H_{c2}^{ab}(0) \sim 39$ T, and the out-of-plane superconducting coherence length $\xi_c(0) \sim 28$ Å. Based on the similarities between these ruthenates and the superconductor $\text{YBa}_2\text{Cu}_3\text{O}_{7-\delta}$, we estimated $H_{c2}^c(0) \sim 8$ T and $\xi_{ab}(0) \sim 140$ Å. We used these parameters to discuss the coexistence of long-range magnetic order and superconductivity on a microscopic scale on these materials.

DOI: 10.1103/PhysRevB.66.144503

PACS number(s): 74.72.-h, 74.25.Ha, 74.62.-c

I. INTRODUCTION

In light of the recent observation of superconductivity at moderately high temperatures, much attention has been devoted to the superconducting properties of the $M(R_{1-x}\text{Ce}_x)_2\text{Sr}_2\text{Cu}_2\text{O}_{10-\delta}$ ($M = 1222; M = \text{Ru}, \text{Nb}, \text{and Ta}; R = \text{Gd}, \text{Eu}$) phase.^{1,2} The Ru-1222 phase crystallizes in a tetragonal structure, space group $I4/mmm$, and it evolves from the Y-123 $R\text{Ba}_2\text{Cu}_3\text{O}_{7-\delta}$ structure by substitution of a fluorite-type layer $(R_{1-x}\text{Ce}_x)_2\text{O}_2$ for the R layer in the 123-type compound. The hole doping of the CuO_2 planes results in metallic behavior and superconductivity (SC) at low temperatures when properly oxidized.^{1,2} It is remarkable that SC occurs in spite of the onset of weak ferromagnetism (wFM) of the Ru sublattice, at a temperature much higher than the superconducting transition temperature T_c . More recently, Felner and co-authors³ have suggested that these two phenomena coexist over a wide range of temperatures in compounds with stoichiometry close to $\text{Ru}(R_{1-x}\text{Ce}_x)_2\text{Sr}_2\text{Cu}_2\text{O}_{10-\delta}$ ($R = \text{Gd}$ and $\text{Eu}; x \sim 0.25$). They found that weak ferromagnetism wFM develops below $T_M \sim 180$ K and 120 K for Gd and Eu compounds, and that the values of T_c were 42 K and 32 K, respectively. This kind of coexistence is a fundamental problem that has been studied both experimentally and theoretically since the early 1960s.⁴ Further evidence that the magnetic ordering is associated with the Ru sublattice and not with the rare earth is provided

by the Ru-NMR and Cu-NMR (nuclear-magnetic-resonance) data on the related compound $\text{RuSr}_2\text{YCu}_2\text{O}_{8-\delta}$, which has a $T_c \sim 45$ K and $T_M \sim 150$ K.⁵ When investigating the coexistence of magnetism and superconductivity in these Ru-based materials, a few points must be taken into consideration. The first point concerns the homogeneity of these solid solutions. Although a number of studies addressing the phase composition of these Ru-based materials is limited, a discussion of whether both the SC and the wFM arise from the same crystallographic phase, and that they coexist on a microscopic scale is in order. One of the first systematic studies on these materials have showed that both phases, the Ru-1222 and the Ru-1212, $\text{RuSr}_2\text{RCu}_2\text{O}_{8-\delta}$ ($R = \text{Sm}, \text{Eu}, \text{and Gd}$), were stable and resulted in nearly single-phase materials after being properly synthesized.² More recently, neutron powder-diffraction analysis of $\text{RuSr}_2\text{GdCu}_2\text{O}_{8-\delta}$ suggested that these materials are comprised of two different domains of orientation of the RuO_6 octahedra, and that the degree of ordering depends on the annealing conditions of the sample.⁶ Results of high-resolution transmission electron microscopy (HRTEM) suggest that the typical extent of the domains is in the 50–200 Å range.⁷ The second point concerns the bulk properties of both the superconducting and the weak-ferromagnetic phases. It is important that to characterize these two phenomena as coexisting, not only superconductivity but also magnetism should develop over a large scale. Although not distinguishing between the two-types of RuO_6

orientation domains, results of scanning tunneling spectroscopy in $\text{RuEu}_{1.5}\text{Ce}_{0.5}\text{Sr}_2\text{Cu}_2\text{O}_{10-\delta}$, combined with macroscopic measurements of magnetization and electrical resistivity, suggest that the SC and wFM are both bulk effects intrinsic to the phase.³ A similar conclusion was also found for the Ru-1212 compounds from specific-heat⁸ and magnetization data.⁹ However, the magnetization data of the Ru-1222 phase reveal that the Ru sublattice generates an internal field of a few hundreds oersteds in the material below the magnetic ordering temperature T_M .³ Such an internal field, higher than the lower thermodynamic critical field H_{c1} , was suggested to be responsible for the appearance of a spontaneous vortex phase in the compound.¹⁰ Indeed, it has also been observed that such vortex configuration is preserved even under an external field as high as 50 Oe. This observation suggests that full Meissner response is difficult to be observed in these materials and that granularity effects, resulting from a mixture of SC and wFM phases, should be absent.³

In this work we describe our investigation of the superconducting $\text{RuGd}_{1.4}\text{Ce}_{0.6}\text{Sr}_2\text{Cu}_2\text{O}_{10-\delta}$ compound synthesized through a sol-gel route and annealed in oxygen pressures as high as 95 atm. Our measurements of magnetization, electrical resistance, and magnetoresistance in applied magnetic fields of 18 T enabled us to determine several parameters of this compound including the temperature dependence of H_{c2} , $H_{c2}(0)$, and estimates of the anisotropic superconducting coherence lengths of these ruthenates.

II. EXPERIMENTAL PROCEDURE

Polycrystalline samples with nominal composition $\text{RuGd}_{1.4}\text{Ce}_{0.6}\text{Sr}_2\text{Cu}_2\text{O}_{10-\delta}$ (Ru-1222) were prepared by the sol-gel method.¹¹ The stoichiometric cationic nitrates and in the case of ruthenium, the chloride, were dissolved in distilled water using a magnetic stirrer. Upon complete dissolution, citric acid in twice the number of total cation moles was added to the solution followed by the same number of moles of ethylene glycol. The solution was then carefully concentrated to $\sim 30\%$ of its original volume, transferred to a ceramic crucible, and evaporated to dryness near 80°C , after which the crucible was heated stepwise to 800°C . The solid black powder residue was then ground, transferred to a ceramic boat, and subjected to two heat treatments in O_2 flow: (1) at 1000°C for 12 h, followed by pelletizing; and (2) at 1050°C for 20 h. Samples subjected to these heat treatments are termed the as-prepared ASP samples. A few pieces of the ASP sample were subjected to an additional heat treatment at 800°C under O_2 pressure of 95 atm for 24 h. These samples are referred to as 95-atm samples. Finally, some parallelepiped bars of the 95-atm samples were subjected to the same heat treatment performed at 800°C and under O_2 pressure of 95 atm for an additional 24 h. These samples are referred to as 95-atm-2X. Further details of the apparatus used for preparing samples under high O_2 pressure can be found elsewhere.¹² The phases were identified by means of powder x-ray diffractometry (XRD) using $\text{Cu } K\alpha$ radiation on a Bruker D8 advanced diffractometer. The lattice parameters were obtained from the corrected peak positions, using MgO

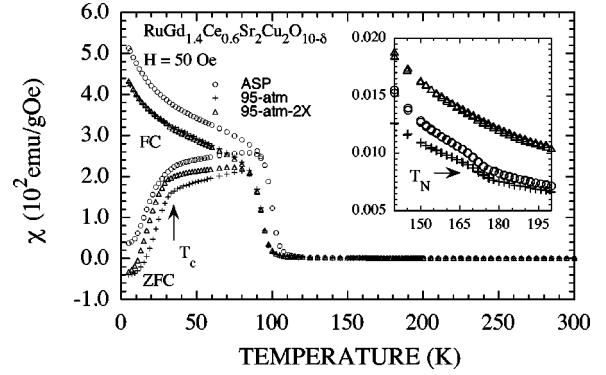


FIG. 1. Curves of magnetic susceptibility χ as a function of temperature taken at $H = 50$ Oe in three specimens of $\text{RuGd}_{1.4}\text{Ce}_{0.6}\text{Sr}_2\text{Cu}_2\text{O}_{10-\delta}$: ASP, annealed at 95 atm of O_2 for 24 h once (95 atm) at 800°C , and twice (95-atm-2X). Both ZFC and FC data were taken. The inset shows the anomalies at ~ 175 K, which can be associated with the onset of antiferromagnetic ordering within the RuO_2 planes.

as an internal standard. The XRD spectra for all samples could be indexed according to a tetragonal structure with space group $I4/mmm$ and lattice parameters $a = 3.835 \pm 0.005 \text{ \AA}$ and $c = 28.56 \pm 0.04 \text{ \AA}$, in agreement with previous data.^{1,2} Magnetic-susceptibility measurements were made utilizing a quantum design squid magnetometer. Zero-field-cooled (ZFC) and field-cooled (FC) curves were obtained from 5 to 300 K in applied magnetic fields of 7 T. Four-wire electrical resistance measurements, in the temperature range $2 \leq T \leq 300$ K, at 18 T, were performed at the National High Magnetic Field Laboratory—Los Alamos Facility utilizing a commercial Linear Research (Model LR-700) ac resistance bridge operating at a frequency of 16 Hz. For these measurements, copper electrical leads were attached to Ag film contact pads on parallelepiped-shaped samples using Ag epoxy.

III. RESULTS AND DISCUSSION

The ZFC and FC magnetic-susceptibility (χ) data at $H = 50$ Oe as a function of temperature, for the as-prepared and high O_2 pressure treated samples are shown in Fig. 1. These specimens were all derived from the same original batch of the material. The χ vs T data show both the onset of wFM near $T_M \sim 100$ K and the onset of SC at $T_c \sim 30$ K. The value of T_M is ~ 7 K higher for the ASP specimen, while χ vs T curves for the 95-atm and 95-atm-2X samples are similar down to about 70 K. Below this temperature, the ZFC and FC branches for the three samples split. The ZFC χ vs T data below 30 K show a diamagnetic contribution due to SC, which is absent in the FC data. It is worth mentioning that the diamagnetic signal in the ZFC data is offset by the positive contribution of the wFM to χ . The ZFC and the FC data between T_c and T_M are quite different, and a detailed study of this region is in progress. The shape of the curves below T_c is similar for the three samples. The values of χ for the ASP sample are slightly higher than the values for the high O_2 pressure treated samples by about 70 emu/g Oe, which is

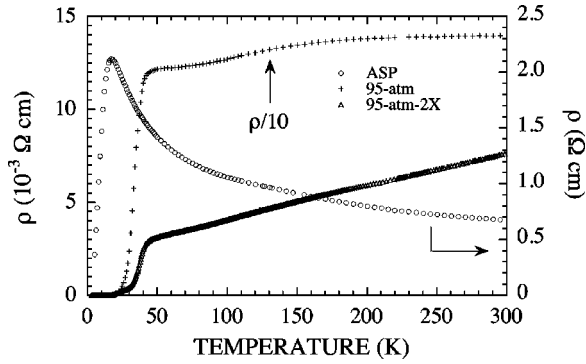


FIG. 2. Temperature dependence of the electrical resistivity for three $\text{RuGd}_{1.4}\text{Ce}_{0.6}\text{Sr}_2\text{Cu}_2\text{O}_{10-\delta}$ samples. The right y axis exhibits the $\rho(T)$ data of the ASP. The left y axis stands for the ones annealed at 95 atm of O_2 at 800°C for 24 h once (95 atm) and twice (95-atm-2X).

essentially the value of the difference in χ of the FC values. The wFM phase originates from an ordered antiferromagnetic state, which develops below $T_N \sim 175$ K.³ The onset of the AF order is accompanied by subtle changes in χ vs T , as indicated in the inset of Fig. 1.

In order to explore further the features observed in the magnetic-susceptibility data, we performed measurements of electrical resistivity as a function of temperature in the same samples of Fig. 1. The temperature dependence of the electrical resistivity $\rho(T)$ for the specimens with the three different treatments is shown in Fig. 2. The $\rho(T)$ data indicate two important features as the sample is heat treated under high pressure of O_2 : (1) an evolution from nonmetallic to metallic behavior; and (2) an appreciable decrease in the magnitude of $\rho(T)$. The changes driven by oxygen treatment are mirrored in the magnitude of $\rho(T=300\text{ K})$, which decreases from ~ 600 m Ω cm for the ASP sample to ~ 130 m Ω cm for the 95-atm specimen. Ultimately, $\rho(T=300\text{ K})$ reaches a value as low as ~ 7 m Ω cm for the 95-atm-2X sample. The value of $\rho(T)$ at 80 K of ca. 3.5 m Ω cm for the latter is nearly twice as small as that by Chen and co-authors,¹³ namely, ca. 6 m Ω cm found in compounds with the same stoichiometry but subjected to heat treatments under 50 atm of O_2 .

Changes in the onset of superconductivity are also observed in our samples with T_c assuming values near 18 K, 42 K, and 42 K for ASP, 95 atm, and 95-atm-2X, respectively. It is clearly seen that the transitions take place over a wide temperature range. Such a broad superconducting transition width, as large as 15 K, is frequently observed not only in these Ru-based compounds but also in both Nb and Ta isomorphous materials.^{1,2} It has been argued that broad transition widths would be mainly associated with cation disorder.¹ This is an important point because one could speculate that larger transition widths could be related to the competition between SC and wFM. However, larger transition widths have been also observed in Nb- and Ta-based compounds which are not magnetic, supporting the conjecture that the broad transitions are intrinsic to compounds with cation disorder.

The evolution of nonmetallic to metallic behavior as the

samples are treated in higher O_2 pressure for a longer time is accompanied by: (1) a progressive increase of the slope $d\rho(T)/dT$; and (2) a sharper transitions to the SC state, both of which can be associated with a reduction of the cation disorder upon oxygenation. The oxygenation process ultimately produces a metal-like material in which $\rho(T) = \rho_0 + AT$, as for example in the sample 95-atm-2X above T_c , where $\rho_0 = 2.2$ m Ω cm and $A = 1.72 \times 10^{-5} \Omega \text{ cm K}^{-1}$. Assuming that the linear dependence on T is caused by electron-phonon (e - p) scattering, the e - p coupling constant λ_{tr} can be estimated from the slope A by utilizing the expression¹⁴

$$\lambda_{tr} = \frac{\hbar \omega_p^2}{8 \pi^2 k_B} \frac{\rho(T) - \rho_0}{T} = \frac{\hbar \omega_p^2}{8 \pi^2 k_B} A, \quad (1)$$

where k_B is the Boltzmann constant, $\hbar \omega_p$ is the plasma energy expressed in eV, and A is expressed in $\mu\Omega \text{ cm K}^{-1}$.

Assuming that the London penetration depth λ_L of our samples is ca. 1 μm ,^{9,15} similar to that obtained for Ru-1212 compounds, the plasma frequency can then be calculated from $\omega_p = c/\lambda_L$, where c is the speed of light, yielding $\hbar \omega_p \sim 0.2$ eV, in excellent agreement with values of $\hbar \omega_p$ found in several cuprates.¹⁴ We are now ready to determine λ_{tr} from the linearity of our $\rho(T)$ data for the 95-atm-2X sample by using Eq. (1). The result is $\lambda_{tr} \sim 0.17$. This value of λ_{tr} is close to the values 0.1 and 0.3 calculated for $\text{La}_{1.85}\text{Sr}_{0.15}\text{CuO}_{4-\delta}$ (LSCO) and $\text{YBa}_2\text{Cu}_3\text{O}_{7-\delta}$, respectively,¹⁴ and it suggests that the electron-phonon coupling in the Ru-based compounds is weak. The value of λ_{tr} should be similar for the samples with the other two heat treatments as well. However, our analysis cannot be extended to the samples that do not show a linear behavior of ρ vs T .

Back to the 95-atm-2X sample, the $\rho(T)$ data do not exhibit any sign of saturation up to 300 K, as shown in Fig. 2, suggesting that the mean free path l is much longer than the interatomic spacing within the unit cell below this temperature. An estimate of the lower limit of the mean free path l at temperatures in which $\rho(T)$ is linear in temperature can be obtained from the expression [Ref. 14]

$$l = \frac{4.95 \times 10^{-4} v_F}{(\hbar \omega_p)^2 \rho}, \quad (2)$$

where v_F is the Fermi velocity, assumed here to be 2.5×10^7 cm/s,^{16,17} and ρ is given in $\mu\Omega \text{ cm}$. The value of l at 300 K from Eq. (2) was found to be ~ 58 \AA , which is over 30 times larger than the typical Cu-O bond length of ~ 1.9 \AA in these materials. This estimate of l (300 K) is also similar to the one of ~ 56 \AA found in LSCO and comparable to other high- T_c cuprates.¹⁴ In light of the evolution of ρ vs T , from being almost temperature independent above T_M for the 95-atm sample, to developing a metal-like slope for the 95-atm-2X sample, we have also estimated l at 300 K by using Eq. (2) for the sample at 95 atm. Our estimate of $l \sim 3$ \AA strongly suggests that the mean free path at high temperatures is comparable to either the typical Cu-O bond

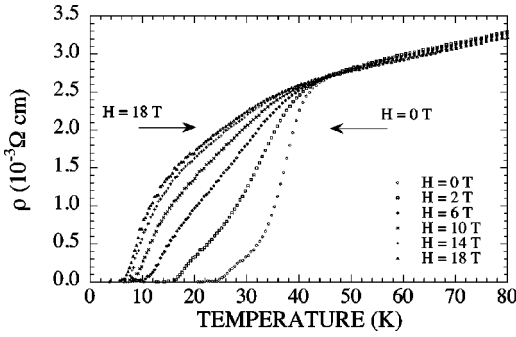


FIG. 3. Temperature dependence of the electrical resistivity under applied magnetic fields up to 18 T for the $\text{RuGd}_{1.4}\text{Ce}_{0.6}\text{Sr}_2\text{Cu}_2\text{O}_{10-\delta}$ compound heat treated in 95 atm of O_2 for 48 h (95-atm-2X).

length ($\sim 1.9 \text{ \AA}$) or the in-plane lattice parameter $a \sim 3.8 \text{ \AA}$. This result has indicated that the saturation of ρ vs T occurs when $l \cong a$, a feature observed in the 95-atm sample, as shown in Fig. 2. Thus, combining the resulting estimates of l from the linearity of ρ vs T curves, we infer that increasing O_2 pressure results in a significant increase of l in this series. This is consistent with a systematic decrease of the cation disorder upon oxygenation, but also with an increasing volume fraction of the metallic phase. Finally, a careful inspection of the data in Fig. 2 for both high-pressure annealed samples also indicates a slight drop in $\rho(T)$ just below T_M ($\sim 100 \text{ K}$), which is probably due to the suppression of the spin-flip scattering below the onset of wFM ordering.

In order to probe the effect of the magnetic field on the superconducting properties of these Ru compounds, we carried out magnetoresistivity measurements in fields up to 18 T. We shall start this discussion by describing the behavior of the curves of $\rho(T)$ in magnetic fields taken in the 95-atm-2X sample, as shown in Fig. 3. It is important to notice that the foot that develops as ρ approaches zero, when $H=0 \text{ T}$, can be due to the remnant field of the superconducting magnet, which is not homogeneous and of the order of 0.01 T in our instrumentation. This kind of behavior is frequently observed in granular superconductors and can account for the broadening of the SC transition at low H and close to the zero-resistance state.¹⁸ In addition, as shown by Tokunaga and co-authors,⁵ it is possible that the broadening of the SC transition could be due to the presence and motion of self-induced vortices. They found that a broad resistive transition in $\text{RuSr}_2\text{YCu}_2\text{O}_8$, a material with no magnetic rare-earth ions, was correlated with the occurrence of the development of a spontaneous moment within RuO_2 planes.

Increasing field results in appreciable changes in the shape of the $\rho(T)$ curves in the superconducting state. As the magnetic field increases, the superconducting transition becomes broader near the onset of SC, and sharper near the zero resistance state, as observed in other granular cuprates.¹⁹ It is important to notice that the zero-resistance state is preserved below 6 K even for the highest magnetic field of 18 T used in this experiment, which attests for the high quality of the high O_2 pressure material obtained.

As an approach to determine the H_{c2} vs T phase diagram,

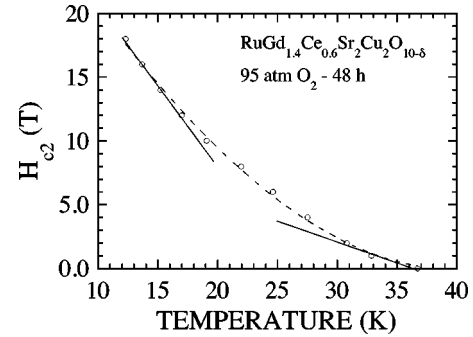


FIG. 4. Temperature dependence of the upper critical field of the magnetic superconductor $\text{RuGd}_{1.4}\text{Ce}_{0.6}\text{Sr}_2\text{Cu}_2\text{O}_{10-\delta}$. The compound was heat treated in 95 atm of O_2 for 48 h (95-atm-2X). The dashed line corresponds to a fit to the phenomenological relation $H_{c2}(T) = H_{c2}(0)[1 - (T/T_c)^2]^\alpha$. The high- and low-field slopes dH_{c2}/dT are also shown in solid lines.

electrical resistivity measurements at constant applied magnetic fields were performed. In Fig. 3, a collection of such data is presented. We fully understand that due to the wide fluctuation regime below T_c , this approach only represents the upper limit in determining H_{c2} values. With this in consideration, we assumed the same onset of SC for all fields ($\sim 42 \text{ K}$) and extracted (H_{c2}, T) pairs from the 50% drops in electrical resistance. The results are displayed in Fig. 4 for the 95-atm-2X sample. At high magnetic fields, the upper-critical-field phase diagram of Fig. 4 shows a linear increase of H_{c2} . This behavior can be attributed to the progressive narrowing of the resistive transition (see data of Fig. 3), which tends to increase $T_c(H)$. The slope of the upper critical field at high fields was found to be -1.13 T/K . At lower fields, the resistive data exhibit an upward curvature developing from a linear slope of -0.38 T/K near $T_c \sim 36 \text{ K}$. This positive curvature is reminiscent of other cuprates (Ref. 20), albeit inconsistent with the linear behavior of H_{c2} expected for both Ginzburg-Landau and BCS theories close to T_c . The orbital critical field extrapolated to $T=0 \text{ K}$ from the linear slope at high fields can be estimated by using the Werthamer, Helfand, and Hohenberg²¹ (WHH) formula $H_{c2}(0) = -0.7(dH_{c2}/dT)T_c$, with $dH_{c2}/dT = -1.13$ and $T_c = 39 \text{ K}$, yielding $H_{c2}(0) \sim 31 \text{ T}$. The same procedure applied to the slope at low fields yields to $H_{c2}(0) \sim 9.6 \text{ T}$. However, previous analysis in several cuprates have not shown the concave downward behavior that is expected in H_{c2} on the basis of the WHH formalism. Therefore, an extrapolation from the fitting procedure of the H_{c2} vs T data to the phenomenological relation $H_{c2}(T) = H_{c2}(0)[1 - (T/T_c)^2]^\alpha$ is more appropriate and consistent with the Ginzburg-Landau theory.²² By doing this, we have obtained $T_c \sim 39 \text{ K}$, $\alpha = 1.8 \pm 0.2$, and $H_{c2}(0) \sim 39 \text{ T}$. Values of α , in the 1.5–2.0 range, are frequently observed in other high- T_c materials.²² Also, this magnitude of $H_{c2}(0) \sim 39 \text{ T}$ is slightly higher than that obtained via the WHH formalism but in line with the values for other high- T_c materials with similar T_c 's.²² According to the relation $H_{c2}(0) = \Phi_0/2\pi\xi_0^2$, where Φ_0 is the quantum of magnetic flux and $H_{c2}(0) \sim 39 \text{ T}$, this corresponds to a superconducting coherence length ξ_0

$\sim 28 \text{ \AA}$, which is one order of magnitude larger than the typical Cu-O bond length and comparable to the c -axis lattice parameter of these Ru compounds.

In light of the anisotropic nature of this magnetic superconductor and the high-field procedure to estimate ξ_0 , it is reasonable to expect that the value of H_{c2} reflects the upper critical field parallel to the a - b plane. By assuming the relationship between H_{c2} and ξ for anisotropic superconductors $H_{c2}^{ab}(T) = \Phi_0/2\pi\xi_c^2(T)$, we find $\xi_c(0) \sim 28 \text{ \AA}$, which reflects mainly the CuO_2 out-of-plane superconducting coherence length. Such a superconducting coherence length along the c direction is found to be four times the value of $\xi_c(0) \sim 7 \text{ \AA}$ for $\text{La}_{1.85}\text{Sr}_{0.15}\text{CuO}_{4-\delta}$ with a T_c of $\sim 38 \text{ K}$ (Ref. 22) and about eight times larger than that of $\xi_c(0) \sim 3.4 \text{ \AA}$ for the electron-doped compound $\text{Nd}_{1.85}\text{Ce}_{0.15}\text{CuO}_{4-\delta}$ with $T_c \sim 25 \text{ K}$.²³ Once we have obtained $\xi_c(0) \sim 28 \text{ \AA}$ for the $\text{RuGd}_{1.4}\text{Ce}_{0.6}\text{Sr}_2\text{Cu}_2\text{O}_{10-\delta}$ compound, it is tempting to estimate the in-plane coherence length $\xi_{ab}(0)$. Let us assume that the anisotropy factor $\gamma (= H_{c2}^{ab}/H_{c2}^c \approx \xi_{ab}/\xi_c)$ of Ru-based compounds has an upper limit given by ca. 5 of the $\text{YBa}_2\text{Cu}_3\text{O}_{7-\delta}$ compound. In fact, it is expected that the $\text{RuGd}_{1.4}\text{Ce}_{0.6}\text{Sr}_2\text{Cu}_2\text{O}_{10-\delta}$ compound would have anisotropy slightly smaller than 5, as suggested elsewhere.^{1,2} Thus, assuming $\gamma = H_{c2}^{ab}/H_{c2}^c \sim 5$, one finds $H_{c2}^c(0) \sim 8 \text{ T}$ and $\xi_{ab}(0) \sim 140 \text{ \AA}$. The estimated value of $H_{c2}^c(0)$ is comparable to the $\sim 9.6\text{-T}$ value found from the slope of the (dH_{c2}/dT) behavior at lower magnetic fields, thus lending credence to the assumptions made in our analysis. The estimated in-plane coherence length of $\xi_{ab}(0) \sim 140 \text{ \AA}$ corresponds to over 30 times the spacing between adjacent conducting CuO_2 planes.

The value of $\xi_{ab}(0) \sim 140 \text{ \AA}$ is important for the discussion involving the microscopic scale in which the SC and the wFM can coexist in these ruthenates.^{7,15,24} The results of HRTEM in Ru-1212 of Ref. 7 indicated two different regions or domains with typical dimensions $50 \leq d \leq 200 \text{ \AA}$ in which different orientations of the RuO_6 octahedra are observed. In principle, these two regions may be related to two different phases within grains: one superconducting and another one nonsuperconducting and magnetic, suggesting an intimate mixture of both phases. Thus, assuming that our estimate of $\xi_{ab}(0) \sim 140 \text{ \AA}$ is related to the superconducting phase, this result indicates that superconductivity is limited spatially in a length scale similar to d . Such a coexistence of SC and wFM phases in a submicron length scale resembles the behavior of granular superconductors, and is consistent with several experimental results of these Ru-based compounds.^{6,24,25} On

the other hand, recent magnetization measurements in Ru-1222 indicated that at least two magnetic phases coexist within grains of polycrystalline samples, suggesting a phase separation in these compounds.²⁴ Indeed, it was argued that both phases manifest themselves in a submicron length scale, and would coexist with a superconducting phase. Again, our estimate of $\xi_{ab}(0) \sim 140 \text{ \AA}$ provides a natural length scale for such a coexistence.

Concluding, we have prepared high-quality samples of the magnetic superconductor $\text{RuGd}_{1.4}\text{Ce}_{0.6}\text{Sr}_2\text{Cu}_2\text{O}_{10-\delta}$ through a sol-gel precursor route. The samples with best superconducting and normal-state properties were heat treated under O_2 pressure of 95 atm. The temperature dependence of the magnetic susceptibility showed the development of an antiferromagnetic ordering of the Ru sublattice at $T_N \sim 175 \text{ K}$, which is followed by the onset of weak ferromagnetism near $T_M \sim 100 \text{ K}$. Further decrease in temperature revealed the onset of superconductivity at $T_c \sim 42 \text{ K}$. Measurements of the electrical resistivity as a function of temperature demonstrate the importance of the heat treatment in high pressure of O_2 upon the macroscopic properties of these compounds. From the temperature dependence of magnetoresistivity data, we have estimated the upper limit of the upper critical field along the CuO_2 planes $H_{c2}^{ab}(0) \sim 39 \text{ T}$ and the out-of-plane coherence length $\xi_c(0) \sim 28 \text{ \AA}$. Based on the crystallographic similarities between these Ru-based compounds and the superconductor $\text{YBa}_2\text{Cu}_3\text{O}_{7-\delta}$, we estimated $H_{c2}^c(0) \sim 8 \text{ T}$ and $\xi_{ab}(0) \sim 140 \text{ \AA}$. From these values we were able to discuss the length scale over which superconductivity and magnetism can coexist in these Ru-based compounds.

ACKNOWLEDGMENTS

This work was supported by the Brazilian agency Fundação de Amparo à Pesquisa do Estado de São Paulo (FAPESP) under Grant No. 99/10798-0. Two of us (M.T.E. and V.A.M.) were financially supported by the FAPESP under Grants Nos. 97/11369-0 and 01/03938-2, respectively, and R.F.J. is a Conselho Nacional de Desenvolvimento Científico e Tecnológico (CNPq) fellow under Grant No. 304647/90-0. L.B-D. acknowledges support from the FAPESP under Grant No. 00/07362-5 and from the Sabbatical Fund of the Hebrew University during her stay in São Paulo, where part of this work was carried out. The support of NSF Grant No. INT-9725929 (M.S.T. and A.H.L.) and CNPq (R.F.J.) are gratefully acknowledged. Work at the NHMFL was performed under the auspices of the NSF, the State of Florida, and the U.S. Department of Energy.

*Electronic address: rjardim@if.usp.br

¹R. J. Cava, J. J. Krajewski, H. Takagi, H. W. Zandbergen, R. B. van Dover, W. F. Peck, Jr., and B. Hesse, *Physica C* **191**, 237 (1992).

²L. Bauernfeind, W. Widder, and H. F. Braun, *Physica C* **254**, 151 (1995).

³See, for instance, I. Felner, U. Asaf, Y. Levi, and O. Millo, *Phys. Rev. B* **55**, R3374 (1997); I. Felner, U. Asaf, S. D. Goren, and C. Korn, *ibid.* **57**, 550 (1998); E. B. Sonin and I. Felner, *ibid.* **57**,

R14 000 (1998); I. Felner, U. Asaf, C. Godart, and E. Alleno, *Physica B* **259-261**, 703 (1999); I. Felner, U. Asaf, Y. Levi, and O. Millo, *Physica C* **334**, 141 (2000).

⁴See, for example, *Superconductivity in Ternary Compounds*, edited by M. B. Maple and Ø. Fisher (Springer-Verlag, Berlin, 1982), Vol. II.

⁵Y. Tokunaga, H. Kotegawaw, K. Ishida, Y. Kitaoka, H. Takagiwa, and J. Akimitsu, *Phys. Rev. Lett.* **86**, 5767 (2001).

⁶O. Chmaissem, J. D. Jorgensen, H. Shaked, P. Dollar, and J. L.

- Tallon, Phys. Rev. B **61**, 6401 (2000).
- ⁷A. C. McLaughlin, W. Zhou, J. P. Attfield, A. N. Fitch, and J. L. Tallon, Phys. Rev. B **60**, 7512 (1999).
- ⁸J. L. Tallon, J. W. Loram, G. V. M. Williams, and C. Bernhard, Phys. Rev. B **61**, R6471 (2000).
- ⁹C. Bernhard, J. L. Tallon, E. Brucher, and R. K. Kremer, Phys. Rev. B **61**, R14 960 (2000).
- ¹⁰H. S. Greenside, E. I. Blount, and C. M. Varma, Phys. Rev. Lett. **46**, 49 (1981).
- ¹¹R. F. Jardim, L. Ben-Dor, and M. B. Maple, J. Alloys Compd. **199**, 105 (1993).
- ¹²M. T. Escote, A. M. da Silva, J. R. Matos, and R. F. Jardim, J. Solid State Chem. **151**, 298 (2000).
- ¹³X. H. Chen, Z. Sun, K. Q. Wang, S. Y. Li, Y. M. Xiong, M. Yu, and L. Z. Cao, Phys. Rev. B **63**, 064506 (2001).
- ¹⁴M. Gurvitch and A. T. Fiory, Phys. Rev. Lett. **59**, 1337 (1987).
- ¹⁵B. Lorenz, Y. Y. Xue, R. L. Meng, and C. W. Chu, Phys. Rev. B **65**, 174503 (2002).
- ¹⁶J. Mesot, M. R. Norman, H. Ding, M. Randeria, J. C. Campuzano, A. Paramekanti, H. M. Fretwell, A. Kaminski, T. Takeuchi, T. Yokoya, T. Sato, T. Takahashi, T. Mochiku, and K. Kadowaki, Phys. Rev. Lett. **83**, 840 (1999).
- ¹⁷M. Chiao, R. W. Hill, C. Lupien, L. Taillefer, P. Lambert, R. Gagnon, and P. Fournier, Phys. Rev. B **62**, 3554 (2000).
- ¹⁸R. F. Jardim, L. Ben-Dor, D. Stroud, and M. B. Maple, Phys. Rev. B **50**, 10 080 (1994).
- ¹⁹R. F. Jardim, M. C. de Andrade, E. A. Early, M. B. Maple, and D. Stroud, Physica C **232**, 145 (1994).
- ²⁰G. Blatter, M. V. Feigel'man, V. B. Geshkenbein, A. I. Larkin, and V. M. Vinokur, Rev. Mod. Phys. **66**, 1125 (1994).
- ²¹M. Tinkham, *Introduction to Superconductivity* (McGraw-Hill, New York, 1975).
- ²²*Introduction to Superconductivity and High- T_c Materials*, edited by M. Cyrot and D. Pavuna (World Scientific, Singapore, 1992).
- ²³H. Hidaka and M. Suzuki, Nature (London) **338**, 635 (1989).
- ²⁴Y. Y. Xue, D. H. Cao, B. Lorenz, and C. W. Chu, Phys. Rev. B **65**, 020511 (2001).
- ²⁵Y. Y. Xue, B. Lorenz, R. L. Meng, A. Baikalove, and C. W. Chu, Physica C **364-365**, 251 (2001).